Acta Crystallographica Section F
Structural Biology and Crystallization Communications
ISSN 1744-3091

Improving the diffraction of full-length human selenomethionyl metavinculin crystals by streak-seeding

Erumbi S. Rangarajan and Tina Izard*

Cell Adhesion Laboratory, Department of Cancer Biology, The Scripps Research Institute, Scripps Florida, Jupiter, FL 33458, USA

Correspondence e-mail: mkernick@scripps.edu

Received 7 May 2010
Accepted 12 October 2010

Metavinculin is an alternatively spliced isoform of vinculin that has a 68-residue insert in its tail domain (1134 total residues) and is exclusively expressed in cardiac and smooth muscle tissue, where it plays important roles in myocyte adhesion complexes. Mutations in the metavinculin-specific insert are associated with dilated cardiomyopathy (DCM) in man. Crystals of a DCM-associated mutant of full-length selenomethionine-labeled metavinculin grown by hanging-drop vapor diffusion diffracted poorly and were highly sensitive to radiation, preventing the collection of a complete X-ray diffraction data set at the highest possible resolution. Streak-seeding markedly improved the stability, crystal-growth rate and diffraction quality of DCM-associated mutant metavinculin crystals, allowing complete data collection to 3.9 Å resolution. These crystals belonged to space group $P4_32_12$, with two molecules in the asymmetric unit and unit-cell parameters $a = b = 170$, $c = 211$ Å, $\alpha = \beta = \gamma = 90^\circ$.

1. Introduction

Vinculin, a ubiquitously expressed 117 kDa helix-bundle protein, plays essential roles in stabilizing adhesion complexes, where it provides direct links from the actin cytoskeleton to the extracellular matrix through its interaction with proteins such as talin that bind to integrin receptors (Critchley, 2004). In addition, vinculin also functions as a regulator of adhesion complexes by sensing and translating extracellular mechanical stress (Ziegler *et al.*, 2006; Mierke *et al.*, 2008; Mierke, 2009; Bailly, 2003; Izard & Vonrhein, 2004). Vinculin is held in an inactive closed-clamp conformation through intramolecular, largely hydrophobic, interactions of the C-terminal five-helix-bundle tail (Vt) domain with a compact globular head (VH) domain comprised of three seven-helix bundles (Vh1–Vh3) and a four-helix bundle (Vt2) (Borgon *et al.*, 2004; Bakolitsa *et al.*, 2004). Severing this interaction is required to activate vinculin and this occurs following the binding of activators such as talin or α-actinin to the Vh1 domain, an event that induces conformational changes that displace Vt from a distance (Izard *et al.*, 2004, 2006; Bois *et al.*, 2006; Izard & Vonrhein, 2004; Tran Van Nhieu & Izard, 2007).

Metavinculin (MV) is a muscle-specific alternatively spliced isoform of vinculin that harbors a 68-residue insert in its tail domain. Metavinculin is always co-expressed with vinculin in cardiac and smooth muscle tissue (Belkin *et al.*, 1988) and forms higher order oligomers with vinculin which may be required for its functions (Witt *et al.*, 2004). Critical roles of metavinculin in muscle-tissue homeostasis are suggested by its dynamic regulation in cardiomyocytes, in which mechanical load triggers increases in metavinculin levels, whereas metavinculin levels drop precipitously in spontaneous dilated cardiomyopathy (DCM; Zemljic Harpf *et al.*, 2004). Indeed, targeted deletion of *vinculin* (and thus also *metavinculin*) disables the architecture of costameres and intercalated discs and leads to cardiac failure (Maeda *et al.*, 1997; Olson *et al.*, 2002). Furthermore, there is a striking association of familial and sporadic missense mutations in the *metavinculin* insert in DCM (Olson *et al.*, 2002) and in hypertrophic cardiomyopathy (HCM; Vasile *et al.*, 2006) and these mutations disrupt the unique actin-organizing properties of metavinculin (Olson *et al.*, 2002; Vasile *et al.*, 2006).

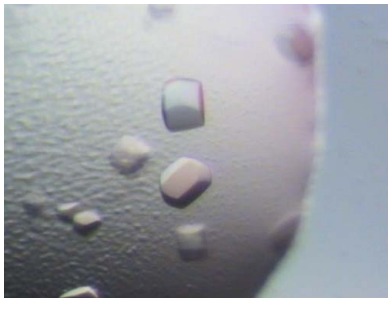

To define how DCM mutations affect metavinculin structure, we crystallized the full-length human ΔLeu954 DCM mutant of human metavinculin by optimizing crystals *via* streak-seeding, which allowed the collection of a complete data set from a single crystal.

2. Materials and methods

2.1. Protein production and crystallization

Full-length selenomethionyl (SeMet) metavinculin-ΔLeu954 (MV-ΔLeu954) protein was overexpressed and purified as described previously for human vinculin (Borgon *et al.*, 2004) except that the lysis buffer was 20 m*M* Tris–HCl pH 7 and 150 m*M* NaCl and a Hi-Trap QHP column (GE Healthcare) equilibrated in 25 m*M* CAPS buffer pH 10 was used for the anion-exchange purification. The protein was concentrated to 22 mg ml^{-1} in 10 m*M* Tris–HCl pH 8 and 1 m*M* DTT.

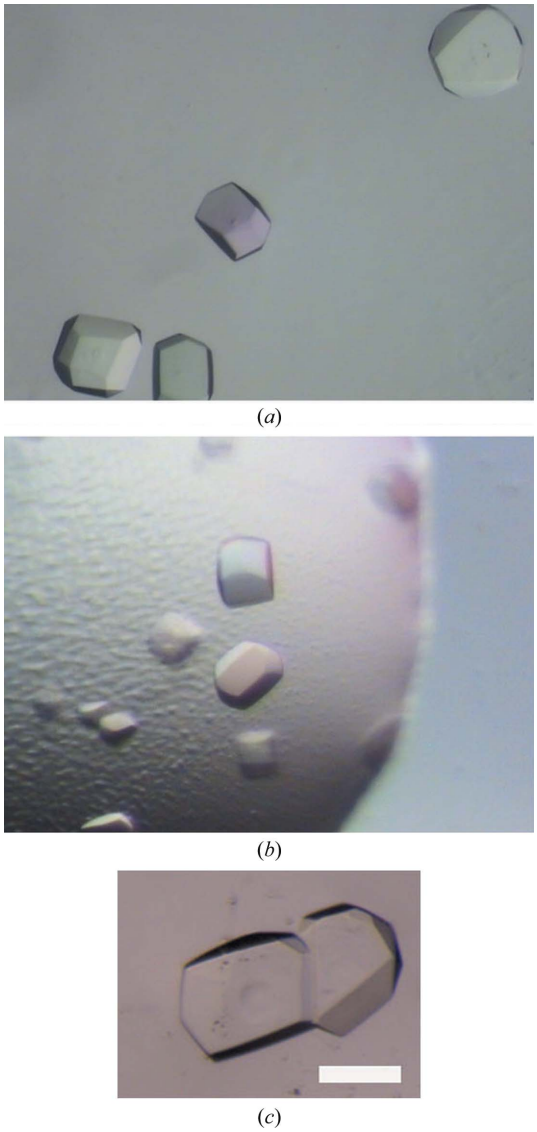

(*a*)

(*b*)

(*c*)

Figure 1
Metavinculin crystals. (*a*) Native full-length human metavinculin-ΔLeu954 crystals. (*b*) SeMet-labeled metavinculin-ΔLeu954 crystals. (*c*) SeMet-labeled metavinculin-ΔLeu954 crystals obtained after streak-seeding. The white bar corresponds to 0.1 mm.

Screening at the Hauptman–Woodward High Throughput Crystallization facility (Luft *et al.*, 2003) identified several initial crystallization conditions at room temperature. After optimization, single crystals were obtained using hanging-drop vapor diffusion from a drop containing equal volumes (0.5 µl each) of protein solution and a reservoir solution consisting of 64 m*M* sodium dihydrogen phosphate, 536 m*M* dipotassium hydrogen phosphate and 175 m*M* ammonium sulfate. SeMet-labeled MV-ΔLeu954 crystals were obtained under identical conditions. To improve these crystals, single SeMet-labeled MV-ΔLeu954 crystals were crushed in 10 µl reservoir solution and used as seeds for streak-seeding with a horse hair into freshly set up drops using the aforementioned reservoir condition at a constant temperature of 295 K.

2.2. X-ray data collection

Prior to data collection, MV-ΔLeu954 crystals were soaked briefly in reservoir solution supplemented with 35%(*v*/*v*) glycerol and flash-cooled in liquid nitrogen. X-ray diffraction data were collected on the SER-CAT (22ID and 22BM) and SBC-CAT (19ID) beamlines at the Advanced Photon Source, Argonne National Laboratory. All data sets were collected at 100 K with 0.5° oscillation and 5–6 s exposure time. Owing to significant radiation damage, an inverse-beam strategy was used for data measured on 22ID with a 5° wedge, which allowed the accurate measurement of Bijvoet differences. All data sets were processed using *autoPROC* (Vonrhein & Bricogne, 2008), which uses an automated procedure for indexing, integration and post-refinement by the program *XDS* (Kabsch, 2010), determination of Laue group and point-group symmetry by *POINTLESS* (Evans, 2006) and determination of the actual resolution of the data through scaling by *SCALA* (Evans, 2006).

3. Results

3.1. Streak-seeding improves crystal quality

Initial crystal optimization trials with native MV-ΔLeu954 mutant protein generated single slow-growing crystals that appeared within 7–10 d and reached a maximum size after one week (0.15–0.2 mm; Fig. 1*a*). SeMet-labeled MV-ΔLeu954 protein was also crystallized similarly. Although these crystals grew to a comparable size within a week, they had a distinct morphology with soft and curved edges (Fig. 1*b*). Interestingly, the morphology of the SeMet-labeled crystals

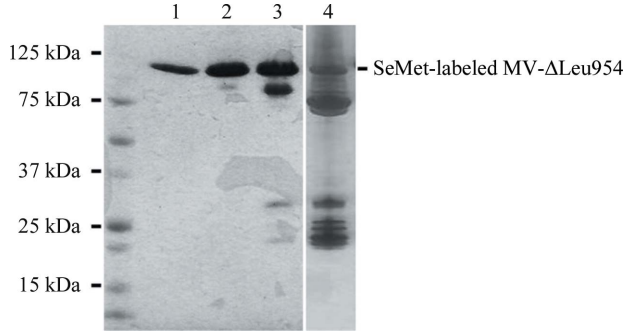

Figure 2
Full-length metavinculin-ΔLeu954 protein is prone to degradation. The protein degrades within a week at room temperature as judged by SDS–PAGE (8–25% gradient) gels. The quality of SeMet-labeled metavinculin-ΔLeu954 protein in solution from streak-seeded crystals from two different drops (lanes 1 and 2) was compared with protein that was left at ambient temperature for 7 d (lane 3) and from crystals that were obtained without streak-seeding (lane 4). Streak-seeding improves crystal quality and stability by accelerating crystal growth. For clarity, the position of the full-length metavinculin mutant protein is indicated.

Table 1
Data-reduction statistics of MV-ΔLeu954 as obtained using *autoPROC* (Vonrhein & Bricogne, 2008).

Values in parentheses are for the last shell.

	SeMet	SeMet, streak-seeded
Beamline	22BM	22BM
Wavelength (Å)	0.97893	0.97893
Space group	$P4_32_12$	$P4_32_12$
Unit-cell parameters		
$a = b$ (Å)	169.8	170.5
c (Å)	210.7	211.1
Resolution (Å)	210.7–6.02 (6.35–6.02)	170.53–3.9 (4.11–3.9)
Total measurements	112716	282414
Unique reflections	8102	27359
Completeness	1.0 (1.0)	0.95 (0.96)
Redundancy	13.9 (14.5)	10.3 (10.4)
$R_{\rm merge}$†	0.084 (0.496)	0.127 (0.486)
$\langle I/\sigma(I)\rangle$	27.2 (6.2)	16.0 (4.8)
Mosaic spread (°)	0.194	0.092

† $R_{\rm merge} = \sum_{hkl}\sum_i |I_i(hkl) - \langle I(hkl)\rangle| / \sum_{hkl}\sum_i I_i(hkl)$.

was improved by streak-seeding, which generated highly reproducible sharp-edged crystals (Fig. 1*c*). Importantly, streak-seeding provided nucleation and accelerated the growth of these crystals, which appeared overnight and reached maximum size (∼0.2 × 0.2 × 0.15 mm) within 3–4 d.

Analysis of the unseeded SeMet-labeled crystals (*i.e.* those grown at a constant temperature of 295 K and harvested after a week of nucleation) by SDS–PAGE showed degradation of the full-length protein (Fig. 2). Additionally, SeMet-labeled MV-ΔLeu954 protein in solution (incubated for one week at ambient temperature) was also very prone to degradation (Fig. 2), suggesting that the delayed appearance of crystals may lead to the incorporation of a heterogeneous population of metavinculin species in the crystal. However, streak-seeding hastens crystal growth, thus allowing the crystals to grow to maximum size prior to protein degradation in the crystallization drop. This is supported by the SDS–PAGE analysis of these crystals, which showed no degradation of the full-length protein (Fig. 2).

3.2. Streak-seeding stabilizes DCM mutant metavinculin

The majority of SeMet-labeled MV-ΔLeu954 crystals diffracted to only about 6 Å resolution, although some (∼10%) initially diffracted to ∼4.0 Å Bragg spacing but the diffraction rapidly decayed after a few frames. After screening several crystals, spanning several synchrotron trips, a data set to 6 Å Bragg spacing was collected on beamline 22BM (Table 1). These crystals were sensitive to X-rays and displayed the characteristics of severe radiation decay. In contrast, marked improvements in diffraction (3.9 Å) were observed with crystals obtained by streak-seeding (Fig. 3*b*), which resulted in a markedly improved data-set quality (Table 1). Also, streak-seeded crystals were more resistant to radiation decay, such that a complete data set could be collected from a single crystal with more than 95% completeness in the highest resolution shell (Table 1). These observations suggest that SeMet-labeled MV-ΔLeu954 crystals are inherently susceptible to radiation damage and that streak-seeding helps to overcome this effect.

4. Discussion

The obstacles encountered in obtaining good data sets for metavinculin-ΔLeu954 DCM mutant crystals are similar to those experienced with human (Borgon *et al.*, 2004), chicken (Bakolitsa *et al.*, 2004) and turkey gizzard (Kogan *et al.*, 2000) vinculin. These hurdles were not the consequence of specific crystallization conditions: metavinculin crystals were generated in 0.6 *M* sodium/potassium phosphate and 175 m*M* ammonium sulfate, those of turkey and chicken vinculin grew in 0.9–1.2 *M* ammonium sulfate (Kogan *et al.*, 2000; Bakolitsa *et al.*, 2004) and human vinculin crystals grew in 10%(*v*/*v*) PEG 2000 (Borgon *et al.*, 2004). Notably, metavinculin and vinculin crystals appear similar in their radiation-sensitivity and are markedly improved by streak-seeding: human vinculin streak-seeded

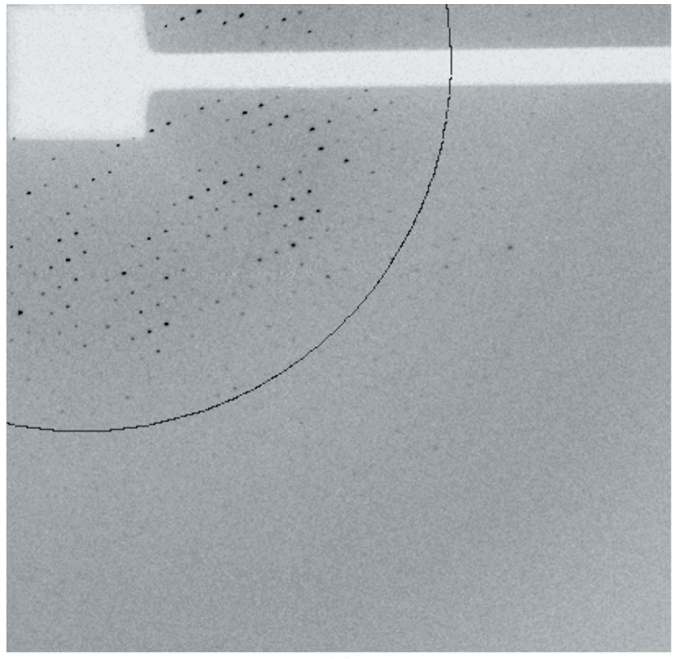

(*a*)

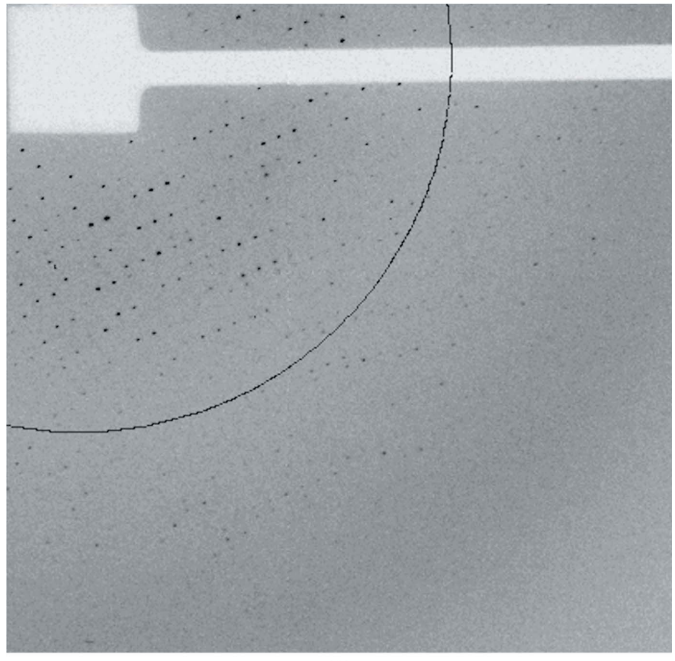

(*b*)

Figure 3
X-ray diffraction images of metavinculin crystals. Diffraction patterns obtained on beamline 22BM at the Advanced Photon Source at Argonne National Laboratory for SeMet-labeled MV-ΔLeu954 mutant crystals grown without streak-seeding (*a*) and obtained through streak-seeding (*b*). Enlarged views of the bottom right quadrants of the images are shown. The ring in both images corresponds to 6 Å.

crystals diffracted to 2.85 Å resolution, while unseeded avian vinculin crystals diffracted to only 3.1 and 3.5 Å resolution despite the fact that these proteins share 99.6% identity and their crystal structures can be superimposed with an r.m.s.d. of 1.4 Å for 741 C^{α} positions. Furthermore, human metavinculin and vinculin streak-seeded crystals overcome degradation as they appeared overnight and achieved their final size shortly thereafter, compared with the 10 d crystal growth without streak-seeding. Likewise, the crystals of turkey gizzard vinculin that diffacted to 3.5 Å resolution took two weeks to attain maximum size (Kogan *et al.*, 2000).

The radiation-sensitive nature of vinculin crystals has been well documented: data sets from several isomorphic human vinculin crystals had to be merged and scaled together to obtain a complete 2.85 Å resolution data set that was suitable for structure determination (Borgon *et al.*, 2004). Furthermore, full-length chicken vinculin was solved at 3.1 Å resolution using modified data-collection strategies such as the collection of MAD data sets at inflection points and high-energy remote wavelengths (Bakolitsa *et al.*, 2004; González *et al.*, 2005), while no structure of turkey vinculin has been reported to date. In all cases, the data collection and structure solution were challenging.

In the present study, metavinculin crystals had characteristics reminiscent of vinculin, especially the SeMet crystals, for which complete data sets could not be collected from single crystals. Indeed, more than 150 metavinculin crystals were screened for X-ray diffraction and this resulted in only nine data sets, none of which produced usable data beyond 5 Å Bragg spacing. Merging partial data sets from multiple crystals was not possible for conventionally grown SeMet-labeled MV-ΔLeu954 crystals as these failed to yield a favorable anomalous signal suitable for substructure determination owing to varying degrees of radiation decay. While the two-wavelength experimental design applied to the chicken vinculin structure facilitated *de novo* phasing (Bakolitsa *et al.*, 2004; González *et al.*, 2005), our data-collection strategy for metavinculin focused on obtaining maximum experimental phasing power without concerns regarding bimodality given the pre-existing vinculin structure. Alternative approaches of data collection through the inverse-beam strategy for accurate measurement of Friedel mates also failed as anomalous completeness in the higher resolution shell was not achieved owing to the extensive radiation damage to the crystals.

Collective approaches, including crystal-manipulation and data-collection strategies, are required to obtain a complete data set from weakly diffracting crystals. A general strategy to overcome radiation damage is to use an X-ray beam such that the radiation dose received by the crystal does not result, over the time scale required to collect a complete data set, in too great a loss in diffraction power or too severe local damage to the anomalous scatterer substructure, as the latter can cause failure to determine this substructure for MAD phasing (Garman, 2010). This can be achieved either by using X-ray sources with a rather limited beam brightness (second-generation synchrotron sources or bending magnets on third-generation sources) or, if the superior optical properties of undulator radiation are desired, by strongly attenuating the beam from such sources. Here, we collected data sets for SeMet-labeled MV-ΔLeu954 DCM crystals using the bending-magnet source (BM-22) at the Advanced Photon Source. Although the approach was effective in reducing radiation damage, only a low-resolution (∼6.0 Å) data set could be collected, suggesting that SeMet-labeled MV-ΔLeu954 crystals are inherently sensitive to synchrotron radiation. Indeed, no anisotropy was detected as judged by the UCLA anisotropy server (Strong *et al.*, 2006), ruling out anisotropy as the cause of our observed loss in diffraction quality. However, this hurdle was overcome when streak-seeded SeMet-labeled MV-ΔLeu954 crystals were used for data collection, which dramatically improved the resolution (Fig. 3; Table 1) and allowed us to collect a complete data set from a single crystal. Thus, streak-seeding of SeMet-labeled MV-ΔLeu954 crystals greatly improved the collection of a complete data set at wavelengths that correspond to the Se peak with minimal radiation damage to the crystals.

We are indebted to colleagues at Scripps Florida: Philippe R. Bois for the cloning of metavinculin and metavinculin-ΔLeu954 and for helpful discussions, John L. Cleveland for fruitful discussions and critical review of the manuscript and Zhen Wu for sequencing. We are also indebted to Gerard Bricogne (GlobalPhasing Ltd) for helpful discussions and suggestions during our synchrotron data collection, as well as Clemens Vonrhein for significant help with various aspects of crystallography. We also thank the staff at the Advanced Photon Source, SER-CAT and SBC-CAT for synchrotron support. TI is supported by grants from the National Institutes of Health and by start-up funds provided to Scripps Florida from the State of Florida. This is publication No. 20610 from The Scripps Research Institute.

References

Bailly, M. (2003). *Trends Cell Biol.* **13**, 163–165.
Bakolitsa, C., Cohen, D. M., Bankston, L. A., Bobkov, A. A., Cadwell, G. W., Jennings, L., Critchley, D. R., Craig, S. W. & Liddington, R. C. (2004). *Nature (London)*, **430**, 583–586.
Belkin, A. M., Ornatsky, O. I., Kabakov, A. E., Glukhova, M. A. & Koteliansky, V. E. (1988). *J. Biol. Chem.* **263**, 6631–6635.
Bois, P. R., O'Hara, B. P., Nietlispach, D., Kirkpatrick, J. & Izard, T. (2006). *J. Biol. Chem.* **281**, 7228–7236.
Borgon, R. A., Vonrhein, C., Bricogne, G., Bois, P. R. & Izard, T. (2004). *Structure*, **12**, 1189–1197.
Critchley, D. R. (2004). *Biochem. Soc. Trans.* **32**, 831–836.
Evans, P. (2006). *Acta Cryst.* D**62**, 72–82.
Garman, E. F. (2010). *Acta Cryst.* D**66**, 339–351.
González, A., von Delft, F., Liddington, R. C. & Bakolitsa, C. (2005). *J. Synchrotron Rad.* **12**, 285–291.
Izard, T., Evans, G., Borgon, R. A., Rush, C. L., Bricogne, G. & Bois, P. R. (2004). *Nature (London)*, **427**, 171–175.
Izard, T., Tran Van Nhieu, G. & Bois, P. R. (2006). *J. Cell Biol.* **175**, 465–475.
Izard, T. & Vonrhein, C. (2004). *J. Biol. Chem.* **279**, 27667–27678.
Kabsch, W. (2010). *Acta Cryst.* D**66**, 125–132.
Kogan, O., Yarden, A., Gimona, M., Geiger, B. & Safro, M. (2000). *Acta Cryst.* D**56**, 1055–1057.
Luft, J. R., Collins, R. J., Fehrman, N. A., Lauricella, A. M., Veatch, C. K. & DeTitta, G. T. (2003). *J. Struct. Biol.* **142**, 170–179.
Maeda, M., Holder, E., Lowes, B., Valent, S. & Bies, R. D. (1997). *Circulation*, **95**, 17–20.
Mierke, C. T. (2009). *Cell Biochem. Biophys.* **53**, 115–126.
Mierke, C. T., Kollmannsberger, P., Zitterbart, D. P., Smith, J., Fabry, B. & Goldmann, W. H. (2008). *Biophys. J.* **94**, 661–670.
Olson, T. M., Illenberger, S., Kishimoto, N. Y., Huttelmaier, S., Keating, M. T. & Jockusch, B. M. (2002). *Circulation*, **105**, 431–437.
Strong, M., Sawaya, M. R., Wang, S., Phillips, M., Cascio, D. & Eisenberg, D. (2006). *Proc. Natl Acad. Sci. USA*, **103**, 8060–8065.
Tran Van Nhieu, G. & Izard, T. (2007). *EMBO J.* **26**, 4588–4596.
Vasile, V. C., Will, M. L., Ommen, S. R., Edwards, W. D., Olson, T. M. & Ackerman, M. J. (2006). *Mol. Genet. Metab.* **87**, 169–174.
Vonrhein, C. & Bricogne, G. (2008). *Acta Cryst.* A**64**, C78.
Witt, S., Zieseniss, A., Fock, U., Jockusch, B. M. & Illenberger, S. (2004). *J. Biol. Chem.* **279**, 31533–31543.
Zemljic Harpf, A. E., Ponrartana, S., Avalos, R. T., Jordan, M. C., Roos, K. P., Dalton, N. D., Phan, V. Q., Adamson, E. D. & Ross, R. S. (2004). *Am. J. Pathol.* **165**, 1033–1044.
Ziegler, W. H., Liddington, R. C. & Critchley, D. R. (2006). *Trends Cell Biol.* **16**, 453–460.